All Sciences Proceedings

5th International Conference on Applied Engineering and Natural Sciences

July 10-12, 2023 : Konya, Turkey

All Sciences Proceedings
http://as-proceeding.com/

https://www.icaens.com/

Single-Flow Supercritical CO_2 Brayton Cycles: A Performance Comparison of the Different Layouts

Serpil ÇELİK TOKER*[1], Önder KIZILKAN [1]

[1]Mechanical Engineering/Isparta University of Applied Sciences, Turkey

*serpilcelik@isparta.edu.tr

Abstract – Supercritical CO_2 Brayton cycle (sCO_2-BC) has been frequently used in power generation applications in recent years due to its high efficiency, compact size, and low-cost advantages. In this study, performances of different configurations of single-flow sCO_2-BCs, such as recuperation, intercooling, reheating, pre-compression, inter-recuperation, and split expansion, are examined. Firstly, thermodynamic analyzes of six different single-flow sCO_2-BCs were conducted. Secondly, parametric analyses based on the system performance-influencing parameters, such as turbine input temperature, turbine inlet pressure, and compressor inlet pressure, were carried out. Engineering Equation Solver (EES) computer software was used in the analysis. According to the initially accepted design parameters, the highest energy efficiency was calculated as 39.25 % in the reheating cycle, and the lowest efficiency was found as 29.62 % in the split expansion BC. Moreover, it has been determined that the energy and exergy efficiencies of cycles increase with rising turbine input temperature and turbine input pressure.

Keywords – Supercritical CO_2, Single-flow CO_2 Brayton cycle, Energy, Exergy

I. INTRODUCTION

CO_2 is a desirable working agent for energy production thanks to its exceptional compressibility, low toxicity, and effective heat transfer [1]. In addition, CO_2 is environmentally friendly and non-flammable. CO_2 has an ODP of 0 and a GWP of 1, and due to its thermal stability, it can be easily used in low and high-temperature heat source applications [2]. In comparison to the traditional Rankine cycle, the sCO_2-BCs are the more advanced power cycles [3]. Near the critical point, CO_2 displays characteristics of both a liquid and a gas. In this case, it has a higher density and specific heat capacity than a gas and a lower viscosity than a liquid. To reduce compressor work, the sCO_2 power cycle makes use of the high compressibility factor and density close to the critical point [4]. Moreover, the sCO_2 power cycle allows for the employment of compact heat exchanger technology and has a more compact turbo-machinery that is just approximately 1/10 the size of a steam Rankine cycle [5]. The CO_2's compressibility factor varies between 0.2-0.5, which allows for a significant reduction in compression work. Additionally, the sCO_2 cycle has the ability to raise the temperature of the turbine inlet since sCO_2 is less corrosive than steam at the same temperature [6]. Superior thermal efficiency, lower greenhouse gas emissions, compact design, cheap capital cost, and other advantages could be offered by sCO_2-BCs in terms of energy, economy, and the environment [7]. SCO_2-BCs can be easily integrated into many applications, such as solar energy [8], geothermal energy [9], nuclear energy [10], and waste heat [11].

Basically, the sCO_2-BC consists of a single flow, split flow, and combined cycles. Various configurations exist in the literature to increase the overall thermal efficiency of sCO_2-BCs [4]. The thermal performance of the sCO_2-BC can be reached by increasing the turbine operating capacity, recovering heat from the recuperator, additional reheating, reducing the compression power, reducing the compressor input temperature, and additional intercooling [12]. Single (non-split) flow configurations are consisted of recuperation,

intercooling, reheating, pre-compression, inter-recuperation, and split expansion cycles. In order to reduce or increase the compression or expansion work intercooling and reheating are used, respectively [4]. More recently, some researchers investigated the sCO_2-BC. Al-Sulaiman and Atif (2015) examined the thermodynamic analysis of various (simple, recuperator, recompression, pre-compression, and split expansion) sCO_2-BC[13]. Ruiz-Casanova et al. (2020) studied the performance and optimization of four various sCO_2-BCs, which are simple, recuperator, intercooling, recuperator, and intercooling. The highest net power (799.99 kW), energy efficiency (11.51%), and exergy efficiency (52.49%) were founded for the Brayton cycle with recuperator and intercooling [9]. Thermodynamic analyses of the recuperator, recompression, pre-compression, intercooling, partial cooling, and split expansion sCO_2-BCs were conducted by Chen et al. (2021) [14]. Sleiti et al. (2021) performed energy and exergy analyses of Brayton cycles in five various layouts, which are recuperator, dual recuperator, intercooling, reheating, and partial intercooling [15]. Wang et al. (2018) compared the performances of five various sCO_2-BCs: solar assisted partial cooling, recompression, pre-compression, intercooling and recuperator. They stated that the highest performance was calculated in the sCO_2-BCs with intercooling and partial cooling [16]. Xingyan et al. (2022) developed dynamic modeling of four various sCO_2-BCs under partial load, recuperator, recompression, reheat and intercooling, and compared the cycles. The thermal efficiency of sCO_2-BCs with reheat, intercooling, recompression and recuperator under the accepted design conditions were found to be 42.35%, 42.04%, 41.66% and 33.54%, respectively [17].

This study is purposed to present a performance comparison of all single flow sCO_2-BCs with different layouts. The single-flow sCO_2-BCs examined consist of six different sCO_2-BCs with recuperation, intercooling, reheating, pre-compression, inter-recuperation, and split expansion. Firstly, the thermodynamic analyzes of six different single-flow Brayton cycles were made using the EES program, and the performances of the cycles were compared. Subsequently, parametric studies have been carried out to examine the impact of turbine input temperature, turbine input pressure, and compressor input pressure on sCO_2-BC performance.

II. DESCRIPTION OF INVESTIGATED CYCLE LAYOUTS AND THERMODYNAMIC ANALYSIS

Fig. 1 displays the schematic configurations of the sCO_2-BC with recuperation (a), intercooling (b), reheating (c), inter-recuperation (d), pre-compression (e), and split expansion (f), respectively. All sCO_2-BCs basically consist of a gas cooler, compressor, recuperator, turbine, and heater.

The performances of the various single-flow sCO_2-BCs are compared using the EES program. The following presumptions are made in order to simplify the thermodynamic analysis:

- It is supposed that all cycles are operating in steady-state circumstances.
- Pressure variations, kinetic, and potential energies are disregarded.
- Each element in the system is adiabatic.
- The compressor inlet temperature is 32 °C, the compressor input pressure is 8000 kPa, and the turbine's inlet pressure is 20000 kPa.
- The isentropic efficiency of the compressor is 89%, the isentropic efficiency of the turbine is 93%, and the efficiency of the recuperator is 95%.

The steady-state mass balance equation is expressed as [18]:

$$\sum \dot{m}_{in} = \sum \dot{m}_{out} \tag{1}$$

Here, $\dot{m}$ is the mass flow ratio. According to Dincer and Rosen [18], the energy equilibrium for the exergy analysis is as follows:

$$\sum \dot{m}_{in} h_{in} + \sum \dot{Q}_{in} + \sum \dot{W}_{in} = \sum \dot{m}_{out} h_{out} + \sum \dot{Q}_{out} + \sum \dot{W}_{out} \tag{2}$$

Here, h is the specific enthalpy, $\dot{Q}$ is the heat transfer rate, and $\dot{W}$ is the work rate. For the exergy analysis, the exergy equilibrium is determined as [18]:

$$\sum \dot{m}_{in} ex + \sum \dot{E}x_{in}^{Q} + \sum \dot{E}x_{in}^{W} = \sum \dot{m}_{out} ex + \sum \dot{E}x_{out}^{Q} + \sum \dot{E}x_{out}^{W} + \dot{E}x_{dest} \tag{3}$$

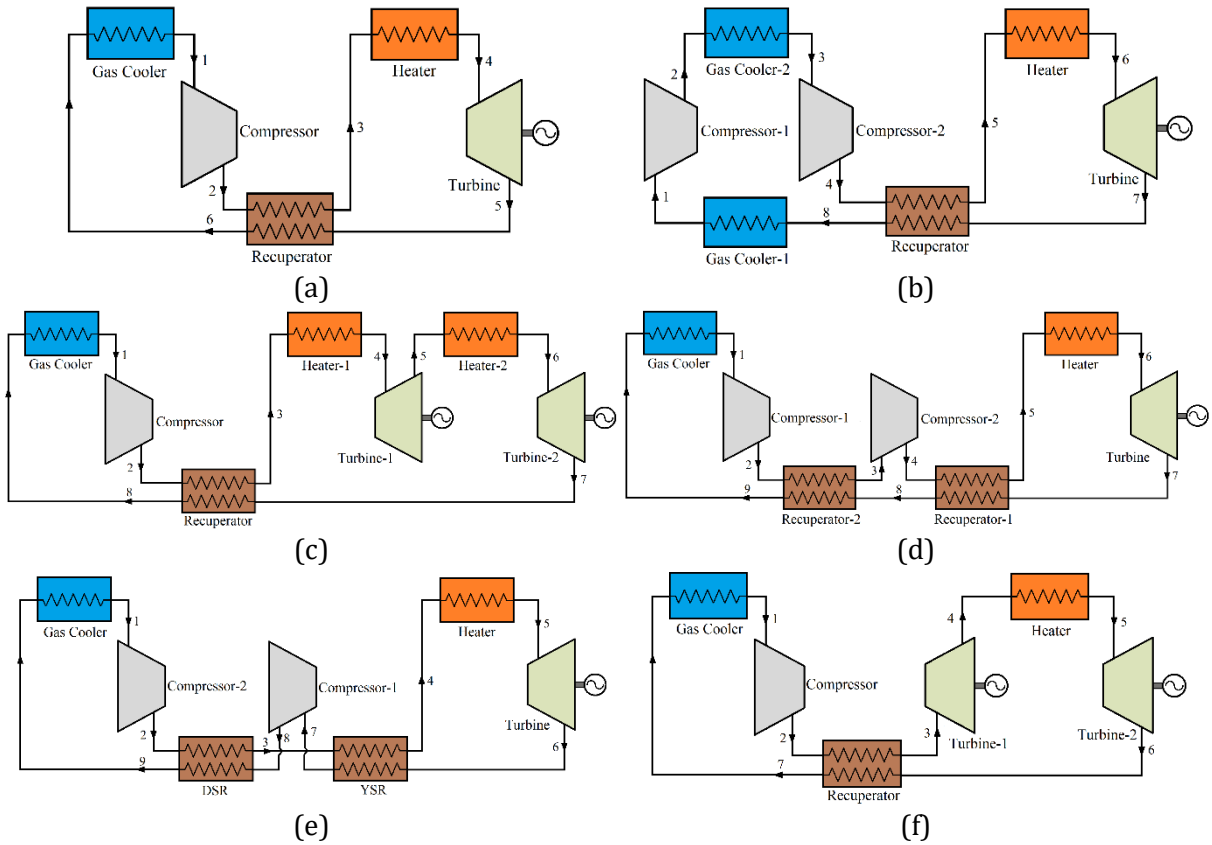

Fig. 1. Layouts of single-flow sCO_2-BCs: (a) Recuperation, (b) Intercooling, (c) Reheating, (d) Inter-recuperation, (e) Pre-compression, (f) Split expansion

where, ex is the agent's exergy, and $\dot{E}x_{dest}$ is the exergy irreversibility.

The sCO_2-BC's energy and exergy efficiencies can be expressed as follows:

$$\eta_{en} = \frac{\dot{W}_{net}}{\dot{Q}_{in}} \tag{4}$$

$$\eta_{ex} = \frac{\dot{W}_{net}}{\dot{E}x_{\dot{Q}_{in}}} \tag{5}$$

III. Results and Discussion

In this article, the exergy and energy performance of the various single-flow sCO_2-BCs were investigated using EES software. Fig. 2 and Fig. 3 depict the effects of changing turbine input temperature on cycle energy and exergy efficiencies. The energy and exergy efficiencies of all single-flow sCO_2-BCs were raised when the turbine input temperature was raised from 400 °C to 900 °C. The highest energy and exergy efficiencies were calculated in the reheating cycle, while the lowest efficiencies were founded in the pre-compression.

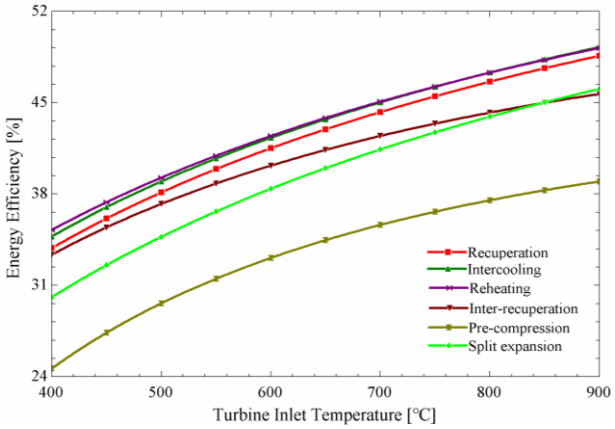

Fig. 2. Variation of energy efficiency with turbine input temperature

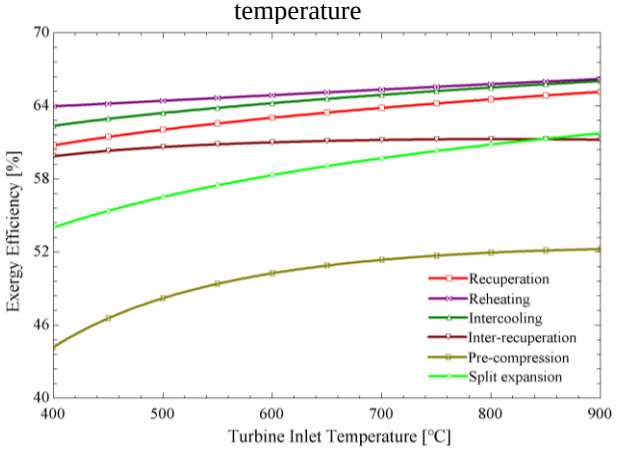

Fig. 3. Variation of exergy efficiency with turbine input temperature

Turbine inlet pressure is another factor that has an impact on system performance. Fig. 4 and Fig. 5 demonstrate the variation of the energy and exergy efficiencies of the cycles with respect to the turbine's input pressure, respectively. As can be seen from Fig. 4 and Fig. 5, the energy and exergy efficiencies of the cycles according to the turbine input pressure increased in the other single-flow sCO_2-BCs, except for the pre-compression cycle. This is because the generated net power increases with the rising turbine's input pressure. The highest energy and exergy efficiencies were calculated in the sCO_2-BCs with intercooling and reheating, and the lowest energy and exergy efficiencies were founded in the sCO_2-BC with pre-compression. The energy and exergy efficiencies of the sCO_2-BC with precompression increased until the turbine input pressure was 20000 kPa and then decreased. The reason for the decrease in energy and exergy efficiencies after 20000 kPa is that the heat rate entering the cycle rises more than the net power.

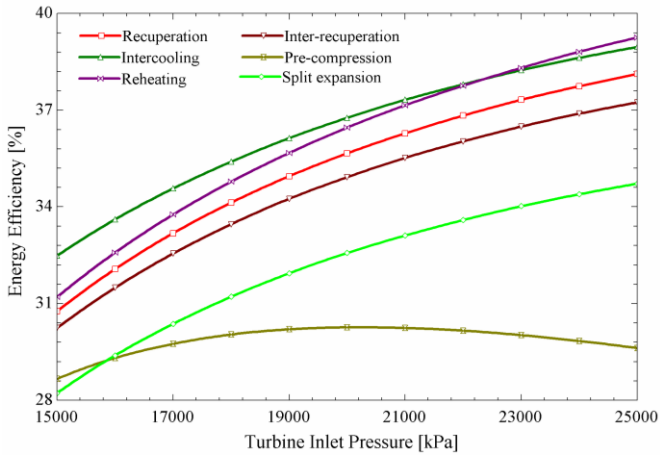

Fig. 4. Variation of energy efficiency with turbine inlet pressure

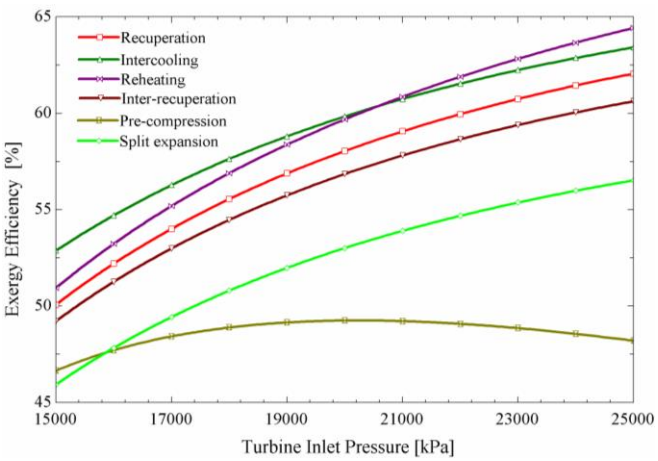

Fig. 5. Variation of exergy efficiency with turbine inlet pressure

Fig. 6 and Fig. 7 manifest the impact of compressor input pressure on the energy and exergy performance of the different single-flow sCO_2-BCs. With the rise of the compressor inlet pressure, the energy and exergy efficiencies of the sCO_2-BCs with recuperation and pre-compression decreased, while the efficiencies of other cycles increased. The reason for the decrease in the efficiencies of the inter-recuperation and pre-compression cycles is the reduction in the amount of heat entering the system according to the rising compressor input pressure.

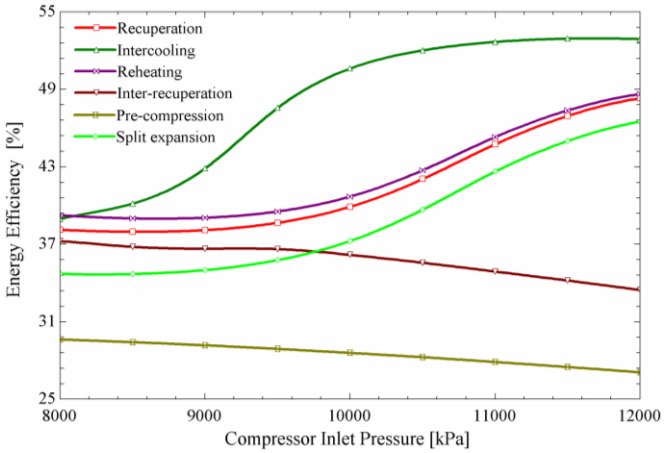

Fig. 6. Variation of energy efficiency with compressor input pressure

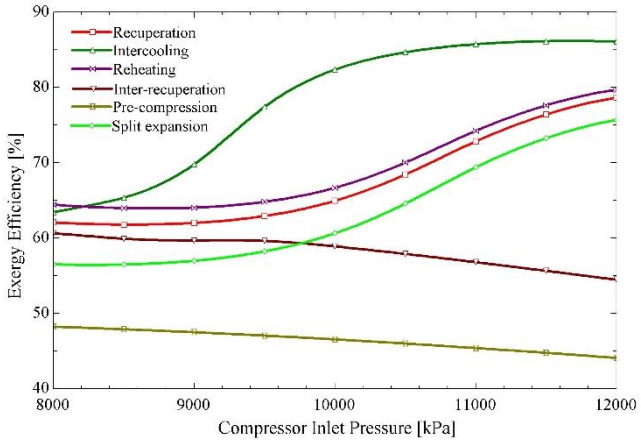

Fig. 7. Variation of exergy efficiency with compressor input pressure

The system operating characteristics were taken into consideration when calculating the energy and exergy efficiency of different single flow sCO_2-BCs. Fig. 8 displays the energy and exergy efficiencies of all single-flow sCO_2-BCs. The highest energy and exergy efficiencies were calculated for the sCO_2-BCs with intercooling and

reheating. It was followed by the Brayton cycle with recuperation, inter-recuperation, split expansion and pre-compression.

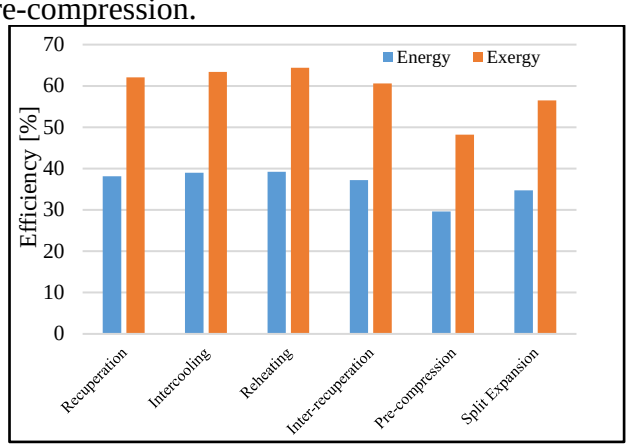

Fig. 8. Energy and exergy efficiencies of various sCO_2-BCs

IV. CONCLUSION

In this paper, a comparative analysis was conducted for the performances of different single-flow sCO_2-BCs (recuperation, intercooling, reheating, inter-recuperation, pre-compression, and split expansion). The mathematical modeling of the studied six different single-flow sCO_2-BCs was established utilizing the EES program. The main parameters used to evaluate the performance of the sCO_2-BCs are turbine input temperature, turbine input pressure, and compressor input pressure. In summary, the results of this paper could be stated as the following:

The energy efficiencies of the sCO_2-BCs with recuperation, intercooling, reheating, inter-recuperation, pre-compression, and split expansion are calculated by 38.12%, 38.96%, 39.25%, %37.24%, 29.62%, and 34.72%, respectively, under design parameters.

The highest exergy efficiency was calculated in the sCO_2-BC with reheating when compared to other single-flow sCO_2-BCs.

The energy and exergy efficiencies of all single-flow sCO_2-BCs increased as the turbine inlet temperature raised from 400 °C to 900 °C.

With the increment of the compressor inlet pressure, the energy and exergy efficiencies of the recuperation and pre-compression sCO_2-BCs reduced, while the efficiencies of the other cycles increased.

As the increase of the compressor inlet pressure, the energy and exergy efficiencies of the sCO_2-BCs with inter-recuperation and pre-compression decreased, while the energy and exergy efficiencies of the other cycles raised.

REFERENCES

[1] E. Jiaqiang *et al.*, "Performance and emission evaluation of a marine diesel engine fueled by water biodiesel-diesel emulsion blends with a fuel additive of a cerium oxide nanoparticle," *Energy Convers. Manag.*, vol. 169, pp. 194–205, Aug. 2018.

[2] J. Huang, A. M. Abed, S. M. Eldin, Y. Aryanfar, and J. L. García Alcaraz, "Exergy analyses and optimization of a single flash geothermal power plant combined with a trans-critical CO2 cycle using genetic algorithm and Nelder–Mead simplex method," *Geotherm. Energy*, vol. 11, no. 1, 2023.

[3] H. Li, Y. Zhang, M. Yao, Y. Yang, W. Han, and W. Bai, "Design assessment of a 5 MW fossil-fired supercritical CO2 power cycle pilot loop," *Energy*, vol. 174, pp. 792–804, May 2019.

[4] Y. Ahn *et al.*, "Review of supercritical CO2 power cycle technology and current status of research and development," *Nucl. Eng. Technol.*, vol. 47, no. 6, pp. 647–661, Oct. 2015.

[5] G. Lv, J. Yang, W. Shao, and X. Wang, "Aerodynamic design optimization of radial-inflow turbine in supercritical CO2 cycles using a one-dimensional model," *Energy Convers. Manag.*, vol. 165, pp. 827–839, Jun. 2018.

[6] G. S. Was *et al.*, "Corrosion and stress corrosion cracking in supercritical water," *J. Nucl. Mater.*, vol. 371, no. 1–3, pp. 176–201, Sep. 2007.

[7] J. M. Cardemil and A. K. Da Silva, "Parametrized overview of CO2 power cycles for different operation conditions and configurations – An absolute and relative performance analysis," *Appl. Therm. Eng.*, vol. 100, pp. 146–154, May 2016.

[8] G. S. Delsoto, F. G. Battisti, and A. K. da Silva, "Dynamic modeling and control of a solar-powered Brayton cycle using supercritical CO2 and optimization of its thermal energy storage," *Renew. Energy*, vol. 206, pp. 336–356, Apr. 2023.

[9] E. Ruiz-Casanova, C. Rubio-Maya, J. J. Pacheco-Ibarra, V. M. Ambriz-Díaz, C. E. Romero, and X. Wang, "Thermodynamic analysis and optimization of supercritical carbon dioxide Brayton cycles for use with low-grade geothermal heat sources," *Energy Convers. Manag.*, vol. 216, p. 112978, Jul. 2020.

[10] J. Syblik, L. Vesely, S. Entler, J. Stepanek, and V. Dostal, "Analysis of supercritical CO2 Brayton power cycles in nuclear and fusion energy," *Fusion Eng. Des.*, vol. 146, pp. 1520–1523, Sep. 2019.

[11] J. Tang, Q. Li, S. Wang, and H. Yu, "Thermo-economic optimization and comparative analysis of different organic flash cycles for the supercritical CO2 recompression Brayton cycle waste heat recovery," *Energy*, vol. 278, p. 128002, Sep. 2023.

[12] Y. Liu, Y. Wang, and D. Huang, "Supercritical CO2

Brayton cycle: A state-of-the-art review," *Energy*, vol. 189. Pergamon, p. 115900, 15-Dec-2019.

[13] F. A. Al-Sulaiman and M. Atif, "Performance comparison of different supercritical carbon dioxide Brayton cycles integrated with a solar power tower," *Energy*, vol. 82, pp. 61–71, Mar. 2015.

[14] R. Chen, M. Romero, J. González-Aguilar, F. Rovense, Z. Rao, and S. Liao, "Design and off-design performance comparison of supercritical carbon dioxide Brayton cycles for particle-based high temperature concentrating solar power plants," *Energy Convers. Manag.*, vol. 232, p. 113870, Mar. 2021.

[15] A. K. Sleiti and W. A. Al-Ammari, "Energy and exergy analyses of novel supercritical CO2 Brayton cycles driven by direct oxy-fuel combustor," *Fuel*, vol. 294, p. 120557, Jun. 2021.

[16] K. Wang, M. J. Li, J. Q. Guo, P. Li, and Z. Bin Liu, "A systematic comparison of different S-CO2 Brayton cycle layouts based on multi-objective optimization for applications in solar power tower plants," *Appl. Energy*, vol. 212, pp. 109–121, Feb. 2018.

[17] B. Xingyan, X. Wang, R. Wang, J. Cai, H. Tian, and G. Shu, "Optimal selection of supercritical CO2 Brayton cycle layouts based on part-load performance," *Energy*, vol. 256, p. 124691, Oct. 2022.

[18] I. Dincer and M. A. Rosen, “Exergy and Energy Analyses,” *Exergy*, pp. 21–30, Jan. 2013.